aerugite are nickel-deficient with a stoichiometry of $Ni_{3.67}As_2O_8$. Charge balance occurs by alternation with cation-deficient $Ni_{4.83}AsO_8$ octahedral layers. An analogous description of the $(Ni,Mg)_{10}Ge_3O_{16}$ structure in terms of $(Ni,Mg)_4Ge_2O_8$ olivine layers and $(Ni,Mg)_6GeO_8$ rock-salt layers (Barbier, 1987*a*) led to the recognition of a new structural family of germanate compounds, $M_{4n+6}Ge_{2n+1}O_{8(n+1)}$ (M = Ni + Mg), of which the members $n = 1$ ($M_{10}Ge_3O_{16}$), $n = 2$ ($M_{14}Ge_5O_{24}$) and $n = \infty$ (M_2GeO_4 olivine) have been identified as stable phases (Barbier, 1987*b*). The structural relationship between aerugite ($Ni_{8.5}As_3O_{16}$ and its Co analogue), xanthiosite ($Ni_3As_2O_8$ and its Co analogue), and the olivine-like phase $Co_{6.95}As_{3.62}O_{16}$ and its possible but as yet unreported Ni analogue, suggest that the nickel and cobalt arsenates (and perhaps the magnesium arsenates) may form a structural series similar to the germanate series, with aerugite and xanthiosite corresponding to the end members $n = 1$ and $n = \infty$, respectively. Indeed, work presently in progress indicates the existence of yet another new nickel arsenate phase with a composition intermediate between those of aerugite and xanthiosite and with unit-cell parameters corresponding to a six-layer close-packed structure, possibly similar to that of the $n = 2$ member of the germanate series, $M_{14}Ge_5O_{24}$ (*cf.* Barbier, 1987*b*).

We thank Y. Le Page and R. E. Marsh for helpful comments, and F. J. Wicks and the Royal Ontario Museum for loan of a sample of natural aerugite. This study was supported by Natural Sciences and Engineering Research Council of Canada operating grants to MEF and JB.

References

BARBIER, J. (1987*a*). *J. Solid State Chem.* **68**, 52–60.

BARBIER, J. (1987*b*). *Acta Cryst.* B**43**, 422–429.

BLESS, P. W. & KOSTINER, E. (1973). *J. Solid State Chem.* **6**, 80–85.

CALVO, C. & FAGGIANI, R. (1975). *Can. J. Chem.* **53**, 1516–1520.

COPPENS, P. & HAMILTON, W. C. (1970). *Acta Cryst.* A**26**, 71–83.

DAVIS, R. J., HEY, M. H. & KINGSBURY, A. W. G. (1965). *Mineral. Mag.* **35**, 72–83.

FLEET, M. E. & BARBIER, J. (1988). *Acta Cryst.* C**44**, 232–234.

GOPAL, R., RUTHERFORD, J. S. & ROBERTSON, B. E. (1980). *J. Solid State Chem.* **32**, 29–40.

International Tables for X-ray Crystallography (1974). Vol. IV. Birmingham: Kynoch Press. (Present distributor Kluwer Academic Publishers, Dordrecht.)

KRISHNAMACHARI, N. & CALVO, C. (1970*a*). *Can. J. Chem.* **48**, 3124–3131.

KRISHNAMACHARI, N. & CALVO, C. (1970*b*). *Can. J. Chem.* **48**, 881–889.

KRISHNAMACHARI, N. & CALVO, C. (1971). *Can. J. Chem.* **49**, 1629–1637.

KRISHNAMACHARI, N. & CALVO, C. (1973). *Acta Cryst.* B**29**, 2611–2613.

KRISHNAMACHARI, N. & CALVO, C. (1974). *Can. J. Chem.* **52**, 46–50.

LE PAGE, Y. (1987). *J. Appl. Cryst.* **20**, 264–269.

SHANNON, R. D. (1976). *Acta Cryst.* A**32**, 751–767.

TAYLOR, J. B. & HEYDING, R. D. (1958). *Can. J. Chem.* **36**, 597–606.

Acta Cryst. (1989). B**45**, 205–212

A Structural Analysis of Barium Magnesium Hollandites

BY ROBERT W. CHEARY AND ROSEANNE SQUADRITO

School of Physical Sciences, University of Technology Sydney, PO Box 123, *Broadway, New South Wales, Australia* 2007

(*Received* 6 *October* 1988; *accepted* 25 *November* 1988)

Abstract

The composition range, lattice parameters and ordering of the Ba ions in the monoclinic hollandite system $Ba_x(Mg_xTi_{8-x})O_{16}$ have been investigated using X-ray powder diffraction data. Rietveld refinement of high-resolution neutron powder diffraction data has also been carried out on the end members $Ba_{1.14}(Mg_{1.14}Ti_{6.86})O_{16}$ and $Ba_{1.33}(Mg_{1.33}Ti_{6.67})O_{16}$. The increasing monoclinic distortion in these compounds with increasing Ba concentration arises from a change in the shape of the **b**-axis tunnels. No significant deformation of the tunnel walls occurs and the cell volume remains constant. The distortion is stabilized in the $x = 1.33$ hollandite by the Mg ions preferentially occupying one particular type of O octahedra. Off-centring of the octahedral cations within the O octahedra appears to reduce the extent of three-dimensional ordering in Ba hollandites. This probably arises because the electrostatic shielding between adjacent tunnels is increased when large dipole moments are set up by off-centre cations in the tunnel walls. Reasonable agreement is obtained between the observed and calculated positons of the X-ray superlattice lines in $Ba_x(Mg_xTi_{8-x})O_{16}$ for $x \leq 1.23$. In the vicinity of $x = 1.33$ the observed 2θ positions differ significantly from the values calculated

0108-7681/89/030205-08$03.00

for the superstructure Ba–Ba–Vacancy expected at this composition. This discrepancy is attributed to the formation of microdomains.

Introduction

Barium hollandites have attracted considerable attention owing to their proposed use in SYNROC. This synthetic mineral is being developed as a host for high-level radioactive waste. Hollandites in particular are included because Cs can be substituted for Ba without any substantial decrease in their resistance to chemical attack (Kesson & White, 1986*a*,*b*). The general unit-cell formula of Ba hollandites is $Ba_x(M_yTi_{8-y})O_{16}$ where $x \leq 2$, and M is either a divalent or trivalent cation, such as Mg^{2+}, Mn^{2+}, Al^{3+} or Ti^{3+}, occupying sites within O octahedra. In the basic tunnel framework formed by the linked O octahedra, the Ba ions occupy sites within the tunnels, and the M and Ti ions occupy sites within the tunnel walls.

In SYNROC the host Ba hollandite is based on a Ti^{3+}/Ti^{4+} cation combination on the octahedral sites. At one extreme, $x \approx 1{\cdot}14$, this hollandite is monoclinic and close to a monoclinic/tetragonal phase boundary, but as x increases the monoclinic distortion becomes more pronounced. The compounds in the present study, $Ba_x(Mg/Ti)O_{16}$, have similar structural characteristics to $Ba_x(Ti^{3+}Ti^{4+})O_{16}$, but are considerably easier to fabricate. Both materials exhibit long-range three-dimensional ordering of the Ba ions and vacant tunnel sites which shows up as well-resolved superlattice lines in electron diffraction patterns (Bursill & Grzinic, 1980; Kesson & White, 1986*a*,*b*). The nature of the ordering changes over the stoichiometry range of these compounds and in most cases is incommensurate. Commensurate superstructures are observed at occupancy levels on the tunnel sites of 60% ($x = 1{\cdot}20$) and 66·67% ($x = 1{\cdot}333$). According to Bursill & Grzinic (1980), $Ba_x(Mg/Ti)$ and $Ba_x(Ga/Ti)$ hollandites are stable over the range $x = 0{\cdot}80$ to $1{\cdot}333$. Mijlhoff, IJdo & Zanderbergen (1985) and Roth (1981) have demonstrated, however, that these hollandites are only stable over the range $x = 1{\cdot}14$ to $1{\cdot}33$. The hollandite structure becomes unstable whenever tunnel sequences form with adjacent vacant sites.

Single-crystal studies of $Ba_x(Mg/Ti)$ hollandites by Dryden & Wadsley (1958) assumed a tetragonal unit cell and the fractional coordinates obtained were similar to those of natural hollandite (Byström & Byström, 1950). They did not recognize, however, that the unit cell is monoclinic. Fanchon, Vicat, Hodeau, Wolfers, Tran Qui & Strobel (1987) have since carried out a single-crystal structure refinement of $Ba_{1{\cdot}20}(Mg_{1{\cdot}20}Ti_{6{\cdot}80})O_{16}$ based on a monoclinic unit cell with ordering of the Ba ions and vacancies included in their model of the structure. Good agreement with the data was obtained by assuming an ordered tunnel structure based on the sequence Ba–Ba–Vacancy–Ba–Vacancy with barium ions next to other bariums occupying off-centre positions, because of the Ba–Ba electrostatic repulsion, and bariums with vacant sites either side occupying a central position. Their X-ray and high-resolution electron microscopy results are consistent with the presence of microdomains in which the structure within each of five possible domains is the same, but in going across a domain boundary there is a shift in the origin of the structure. In their analysis, no ordering on the octahedral sites was detected. Bursill & Grzinic (1980) also observed microdomains <100 Å across in $Ba_{1{\cdot}33}(MgTi)$ hollandite.

In the present work we have established the composition range of the $Ba_x(Mg/Ti)$ hollandites, determined the variation of the lattice parameters over this range, and examined the change in the ordering as reflected by the movement of the superlattice lines in the X-ray powder diffraction data. Rietveld refinement of neutron powder diffraction data has also been carried out on the end-member compounds, $Ba_{1{\cdot}14}(Mg_{1{\cdot}14}Ti_{6{\cdot}86})O_{16}$ and $Ba_{1{\cdot}33}(Mg_{1{\cdot}33}Ti_{6{\cdot}67})O_{16}$, to determine the characteristics of the structural distortion, particularly with respect to the oxygen framework and its embedded octahedral cations. Ordering of the octahedral cations is discussed along with the importance of these ions to the ordering of the tunnel ions.

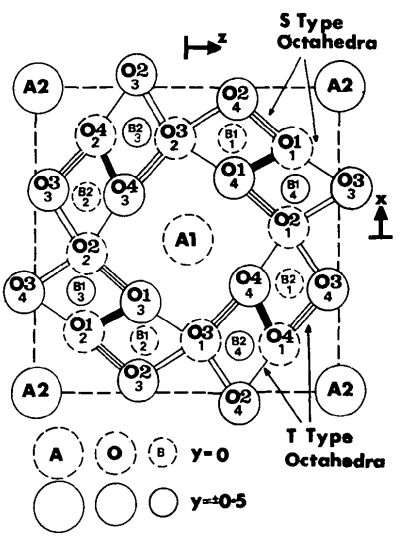

Fig. 1. Projection of the hollandite structure looking down the **b**-axis tunnels showing the various atomic positions referred to throughout the paper. In monoclinic hollandites the oxygen octahedra on opposite sides of the tunnel are identical. The two different types of octahedra are labelled *S* and *T*. The O–O bonds depicted with similar line patterns possess the same bond length in tetragonal hollandites, but in monoclinic hollandites this is only true for opposing sides of the tunnel.

Description of the barium hollandite structure

In monoclinic hollandites described by the space group $I2/m$ the tunnels form along the **b** axis. Fig. 1 represents a projection of the structure looking down the tunnels defining the various oxygen and B sites in the hollandite unit cell, $A_2B_8O_{16}$. The A sites or tunnel sites are only partially occupied by Ba ions and in most cases there is some ordering of these ions and the vacant tunnel sites. Each Ba ion is held within a box-shaped cavity of eight oxygens and can occupy either a central position or one of two possible off-centre positions within the cavity (*i.e.* $0,\pm y,0$ with $y \simeq 0{\cdot}1$ to $0{\cdot}2$). When off-centre the Ba ion makes contact with either the four oxygens, $O1_3$, $O1_4$, $O4_3$ and $O4_4$, at the top of a box ($y = +\frac{1}{2}$) or the equivalent four oxygens at the bottom of a box ($y = -\frac{1}{2}$). The tunnels are defined by oxygen octahedra which form as four walls, hereinafter referred to as the octahedral walls, which are linked together by corner sharing [see illustration in Kesson (1983)]. Each wall consists of two columns of similar octahedra connected by edge sharing and only octahedra on opposite walls have the same dimensions. The structure therefore consists of two different types of octahedra called S and T type as shown in Fig. 1. The B cations in each column of octahedra are shifted off-centre in opposite directions because of the mutual repulsion between the adjacent columns of B ions within a wall.

Specimen preparation and measurement procedures

A series of specimens was prepared to identify the solid-solution range of barium magnesium hollandites $Ba_x(Mg_xTi_{8-x})O_{16}$. The chemistry used to make these compounds is the solid-state reaction of the elemental oxides and carbonates, namely

$$x\mathrm{BaCO_3} + x\mathrm{MgO} + (8-x)\mathrm{TiO_2}.$$

Two reference mixtures corresponding to $x = 1{\cdot}00$ and $x = 1{\cdot}40$ were weighed out (~40 g each), homogenized by wet ball milling for 30 min and dried at 373 K. Precalcine mixtures of approximately 4 g each, suitable for making Ba_x(Mg/Ti) hollandites with $x = 1{\cdot}00$ up to $1{\cdot}40$ in steps of ~0·02, were formed by mixing different proportions of the reference mixtures. All these samples were then homogenized by wet grinding, allowed to dry at 373 K, formed into a pellet and then calcined at 1300 K for about 6 h. After calcining, the specimens were ground up into a fine powder, re-formed as pellets and fired at 1600 K for about 12 h in air. The samples were cooled to approximately 500 K over a period of 24 h before being removed from the furnace.

X-ray powder diffraction data were collected for each of the specimens using Cr $K\alpha$ radiation over the angular range $2\theta = 15$–$110°$. All the specimens displayed well-resolved monoclinic hollandite lines appropriate to the space group $I2/m$ with the monoclinic splitting being more obvious at the larger values of x. Two well-resolved, relatively intense superlattice lines, at $2\theta \simeq 30°$ and $2\theta \simeq 40°$, and a number of less intense superlattice lines arising from the ordering of the Ba ions and vacancies in the tunnels were also present in all the diffraction patterns. Only the second most intense superlattice line can be observed at all x values as the other moves under a lattice line when $x > 1{\cdot}25$. Within the range $x = 1{\cdot}12$–$1{\cdot}34$ all the diffraction lines could be identified and the specimens were essentially single-phase hollandites with both the lattice lines and the superlattice lines shifting uniformly with x. Second-phase lines (*e.g.* TiO_2) were identified outside this range. The large shift in the superlattice lines as the Ba-vacancy ordering changes is a feature of these hollandites. Over the full range of compositions the second strongest superlattice line moves ~3·2° from $2\theta = 28{\cdot}9$ to $32{\cdot}1°$ whereas the 202 lattice line moves only ~0·2° over the same range. The lattice parameters of the hollandites formed were determined by least-squares fitting the 2θ peak positions of the 15 or so well-resolved lattice lines in the angular range measured that could be unambiguously assigned Miller indices.

After identifying the solid-solution range in these hollandites, two further large specimens (~15 g each) with $x = 1{\cdot}143$ and $1{\cdot}333$, were prepared for neutron powder diffraction using the same firing procedures as described earlier. Before measurement these specimens were finely ground in a tungsten carbide ball mill and then annealed at 1200 K. Neutron diffraction data were collected using the high-resolution powder diffractometer at the Australian Nuclear Science and Technology Organisation (ANSTO) at an incident wavelength of 1·377 Å (Howard, Ball, Davis & Elcombe, 1983). All the measurements were carried out at room temperature (298 K) with the specimen compacted into a vanadium can fixed onto the rotating stage of the diffractometer. Each set of data was recorded at fixed monitor counts over an angular range $2\theta = 0$–$150°$ at steps of 0·05°. It is worth noting that unlike the X-ray and electron diffraction patterns, the neutron pattern displays very little evidence of ordering; no superlattice lines are evident.

Structural refinement was carried out by the Rietveld method using the program developed by Wiles & Young (1981) and extensively modified by Howard & Hill (1986). In the present analysis, the diffraction profiles were fitted to a sum of Gaussians (Howard, 1982) and the background was included in the refinement by assuming it could be fitted to a polynomial in 2θ. The non-standard space group $I2/m$ was used to describe the atomic coordinates using the scheme described in Cadee & Verschoor (1978) and Cheary (1986) as this facilitates comparison with tetragonal hollandites. The goodness-of-fit indicators quoted in the results of refinement are defined by Howard & Hill.

Table 1. *Lattice parameters and crystal structure parameters for the barium magnesium hollandites* $Ba_{1\cdot143}(MgTi)_8O_{16}$ *and* $Ba_{1\cdot333}(MgTi)_8O_{16}$ *obtained by Rietveld refinement of neutron powder diffraction data at* 1·377 Å

R_B refers to the Bragg R factor, R_{wp} is the weighted R factor and R_{wp}^{exp} is the best value of the weighted R factor that can be expected on the basis of counting statistics. Also included for comparison are the subcell results for the O atoms and the octahedral ions in $Ba_{1\cdot2}(MgTi)_8O_{16}$ given by Fanchon *et al.* (1987).

	$Ba_{1\cdot14}(Mg_{1\cdot14}Ti_{6\cdot86})O_{16}$				$Ba_{1\cdot33}(Mg_{1\cdot33}Ti_{6\cdot67})O_{16}$				$Ba_{1\cdot20}(Mg_{1\cdot20}Ti_{6\cdot80})O_{16}$		
	x	y	z	B_{iso}	x	y	z	B_{iso}	x	y	z
Ba	0	0·100 (8)	0	3·6 (7)	0	0·155 (3)	0	2·2 (3)	—	—	—
Mg/Ti1	0·3300 (7)	0	0·1513 (8)	0·95 (15)	0·3334 (7)	0	0·1521 (8)	0·57 (18)	0·3347	0	0·1514
Mg/Ti2	0·8516 (7)	0	0·3278 (6)	0·90 (15)	0·8523 (7)	0	0·3269 (6)	0·75 (15)	0·8527	0	0·3312
O1	0·2967 (2)	0	0·3483 (2)	0·68 (8)	0·2948 (2)	0	0·3512 (3)	0·78 (8)	0·2952	0	0·3496
O2	0·0414 (2)	0	0·3283 (2)	0·82 (9)	0·0407 (2)	0	0·3201 (3)	0·86 (8)	0·0413	0	0·3242
O3	0·6607 (2)	0	0·0408 (2)	0·85 (8)	0·6549 (2)	0	0·0403 (2)	0·84 (9)	0·6572	0	0·0410
O4	0·6560 (2)	0	0·3004 (2)	0·69 (8)	0·6588 (3)	0	0·3036 (2)	0·76 (8)	0·6572	0	0·3021
	R_B = 1·8% R_{wp} = 4·5% R_{wp}^{exp} = 2·9%				R_B = 1·8% R_{wp} = 4·8% R_{wp}^{exp} = 2·9%						
	a = 10·1816 (4) Å		b = 2·97330 (7) Å		a = 10·2609 (3) Å		b = 2·98052 (8) Å		a = 10·227 Å		b = 2·9814 Å
	c = 10·0268 (3) Å		β = 90·489 (1)°		c = 9·9212 (3) Å		β = 91·072 (1)°		c = 9·964 Å		β = 90·77°

Excellent fits were obtained to both sets of data. In both cases the known composition was used to fix the occupancy of the bariums on the tunnel sites along with Mg : Ti ratio on the B sites. This was done because the correlation between the temperature factor, the off-centre parameter y and the occupancy of the tunnel sites was too great to obtain physically realistic results from independent refinement of all three parameters. For the same reason dividing the Ba statistically between a central position and an off-centre position and refining the relative occupancy did not prove to be of value. In the structural results given in Table 1 the Mg and Ti distribution on the $B1$ and $B2$ sites was assumed to be random and the same on each type of site. Also included in this table are the subcell results for $Ba_{1\cdot2}(Mg_{1\cdot2}Ti_{6\cdot8})O_{16}$, obtained by Fanchon *et al.* (1987), transformed to the present coordinate system. On the whole their structural coordinates and lattice parameters are similar to the present results. The **b** parameter, however, is greater than both of the present results. This is probably due to the presence of Ti^{3+} ions in their sample which is black rather than colourless as would be the case if only Ti^{4+} and Mg^{2+} ions were present on the octahedral sites. A difference in the **b** parameters would also be expected if the ionic distribution on the octahedral sites was strongly dependent on the heat treatment given to the crystals.

Discussion

The lattice parameters plotted in Figs. 2(*a*), 2(*b*) and 2(*c*) confirm that Ba_x(Mg/Ti) hollandites are stable only over a limited range of compositions. The solid-solution range according to these plots starts between 1·130 and 1·145 Ba per cell [*i.e.* Ba : Mg : Ti $\simeq$ 1 : 1 : 6, x (nominally) = 1·14] and ends between 1·315 and 1·335 Ba per cell [*i.e.* Ba : Mg : Ti $\simeq$ 1 : 1 : 5, x (nominally) = 1·33]. These composition limits have also been observed by Roth (1981). Why hollandites only form over a limited composition range is not clear. Synthetic hollandites with $x < 1$ do not form because pairing of vacant tunnel sites can occur and the structure becomes unstable (Mijlhoff *et al.*, 1985). Additional factors, however, must also affect the lower limit which is $\frac{8}{7}$ in most hollandites rather than 1. The upper limit of x can extend to 1·4 Ba per cell when Ti is replaced by a larger ion such as Sn (Cadee & Verschoor, 1978) and to 1·50–1·54 tunnel ions per cell when Ba is replaced by a monovalent ion such as potassium or caesium (Weber & Schultz, 1986; Kesson & White, 1986*a*,*b*). There is clearly a correlation between the maximum tunnel-site occupancy, the valence of the tunnel ion and the size of the octahedral cation, but the reason for this is not fully understood.

A characteristic of Ba_x(Mg/Ti) hollandites is the cell volume V_c which, to a first-order approximation, does not change with composition (see Fig. 2*d*). This is unusual as most hollandites display a uniform increase in V_c under similar circumstances (Post, Von Dreele & Buseck, 1982; Cheary, 1986). When examined closely there is actually a slight decrease of $\sim 0{\cdot}2$ Å^3 in the present hollandites between $x = 1{\cdot}14$ and 1·33. This can be accounted for by examining the changes in the tunnel volume and the tunnel-wall volume. The volume enclosed within the oxygen octahedra forming the tunnel walls increases from 81·09 to 81·52 Å^3 per unit cell owing to the increased proportion of Mg ions on these sites. The volume enclosed within the hollandite tunnels, however, decreases because of the collapse of the tunnel walls arising from the monoclinic distortion. This is characterized by the volume enclosed by the box of eight oxygens surrounding each tunnel site which drops from 39·00 to 38·79 Å^3 over the composition range. Contraction of the tunnels can occur because none of the oxygens forming the box is in contact with other oxygens. This is evident from the fact that the sides of the box (*i.e.* the O1—O4 distance $\simeq$3·65 Å) are significantly greater than two O^{2-} radii (*i.e.* $\simeq$ 2·6 Å). In addition, the space available within each box of oxygens is not fully occupied by the Ba ions as these

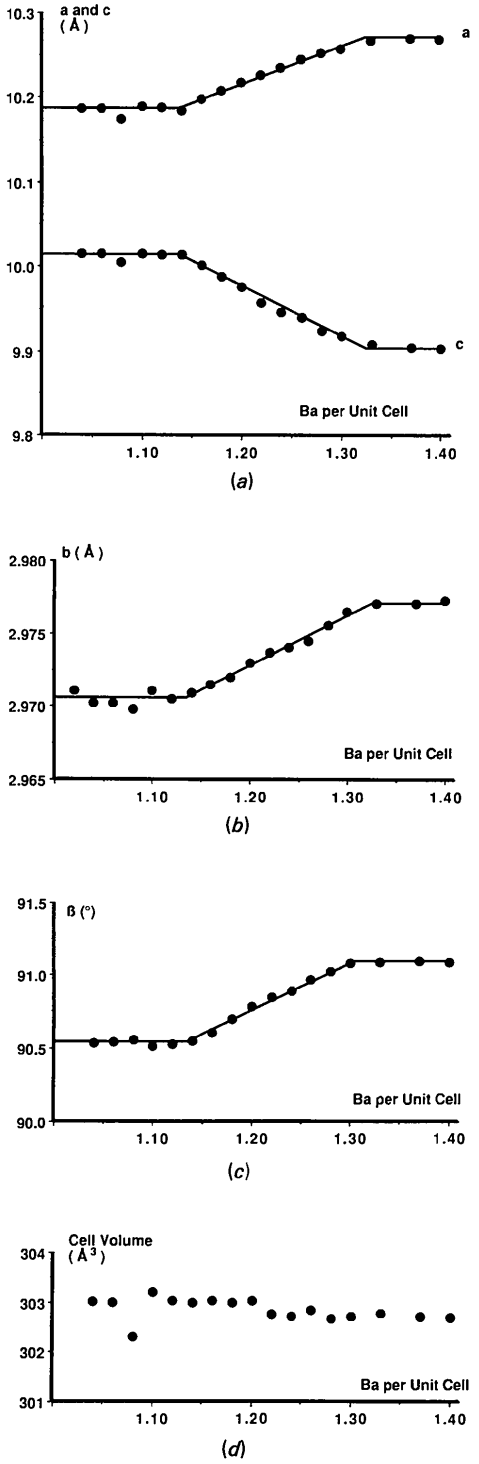

Fig. 2. Lattice parameters (*a*) *a* and *c*, (*b*) *b*, (*c*) β, and (*d*) the cell volume for $Ba_x(Mg_xTi_{8-x})O_{16}$ specimens prepared by the solid-state reaction $x BaCO_3 + xMgO + (8-x)TiO_2$. At $x \leq 1{\cdot}14$ the hollandite formed is always $Ba_{1{\cdot}14}(Mg_{1{\cdot}14}Ti_{6{\cdot}86})O_{16}$ and above $x = 1{\cdot}33$ is always $Ba_{1{\cdot}33}(Mg_{1{\cdot}33}Ti_{6{\cdot}67})O_{16}$. The radiation used is Cr $K\alpha$ and the statistical error in the parameters is smaller than the plotted points [*viz.* $\sigma(a) \approx \sigma(c) \approx 0{\cdot}001$ Å, $\sigma(b) \approx 0{\cdot}0005$ Å and $\sigma(\beta) \approx 0{\cdot}01°$].

cations are off-centre and only in contact with four of the eight oxygens. It should be noted that the off-centre shift of the Ba ions increases from 0·30 (2) Å at $x = 1{\cdot}14$ to 0·46 (1) Å at $x = 1{\cdot}33$. The ordered structure at $x = 1{\cdot}33$ follows the basic sequence Ba–Ba–Vacancy in which all the Ba ions experience off-centring forces. At $x = 1{\cdot}14$, approximately 50% of the Ba ions will be bounded on each side by vacant sites and not experiencing off-centring forces by other tunnel ions. The average off-centre shift will therefore be smaller.

The most significant change in Ba_x(Mg/Ti) hollandites is the development of the monoclinic distortion. The shift of the oxygens forming the tunnel walls going from 1·14 to 1·33 Ba per cell is illustrated in Fig. 3. Broadly speaking, the structure behaves as if hinges exist along axes in the **b** direction through the corner-shared oxygens $O3_1$, $O3_2$, $O2_1$ and $O2_2$. The $O2_1$–$O2_2$ distance decreases by 0·24 Å from 6·63 to 6·39 Å whilst the $O3_1$–$O3_2$ distance increases by 0·18 Å from 6·96 to 7·14 Å. If all the oxygen octahedra forming the walls were similar and expanded uniformly across the solid-solution range and the structure hinged about the four corner-shared oxygens, the changes in the $O2_1$–$O2_2$ and $O3_1$–$O3_2$ distances would be equal and opposite. In actual fact the motion of each tunnel wall over the range $x = 1{\cdot}14$ to 1·33 can be split into three components; expansion due to the changing cation composition, rotation about the hinge axes and a small shear strain with a moment vector in the –**b** direction. Additionally, the *S*- and *T*-type octahedra grow at different rates over the solid-solution range. At the $x = 1{\cdot}14$ end, these octahedra have approximately the same volume and average (Mg/Ti)–O bond length. At the 1·33 end where the Mg concentration is higher, an *S*-type octahedron is larger

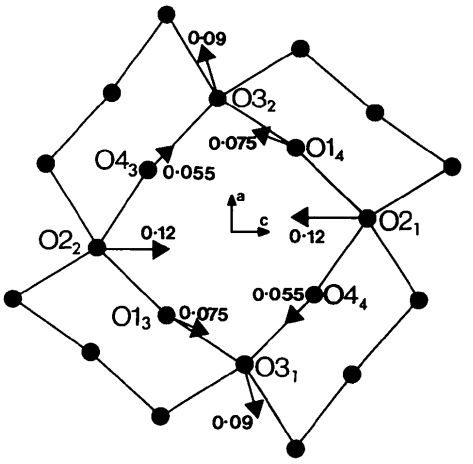

Fig. 3. Shift of the oxygens relative to the tunnel axis going from $Ba_{1{\cdot}14}(Mg_{1{\cdot}14}Ti_{6{\cdot}86})O_{16}$ to $Ba_{1{\cdot}33}(Mg_{1{\cdot}33}Ti_{6{\cdot}67})O_{16}$. The magnitudes (in Å) and directions of the shifts are given on the diagram.

Table 2. *Volumes of the oxygen octahedra in S- and T-type octahedra along with the corresponding average* (Mg/Ti)–O *bond lengths for* $Ba_x(Mg/Ti)_8O_{16}$ *at* $x = 1{\cdot}14$ *and* $1{\cdot}33$

Each bond length quoted under the headings *S* and *T* is an average over the six (Mg/Ti)–O bonds in a particular octahedron.

	Mean Mg/Ti–O bond length (Å)			Oxygen octahedral volume (Å^3)	
x	*S* type	*T* type	Overall	*S* type	*T* type
1·14	1·9756 (8)	1·9759 (8)	1·9757 (8)	10·137 (10)	10·136 (10)
1·33	1·9814 (8)	1·9775 (8)	1·9794 (8)	10·218 (10)	10·162 (10)

than a *T*-type octahedron. The volume of each type of octahedron and the associated (Mg/Ti)–O bond lengths are summarized in Table 2. The errors given in this table are based on the errors in the crystal structure parameters given in Table 1 with allowance being made for correlated parameters.

The different growth rates of the *S* and *T* octahedra suggest that the octahedral cations are not randomly distributed over the two sets of sites. The Mg/Ti–O bond lengths in Table 2 imply that *S*-type octahedra in the 1·33 hollandite contain more Mg than *T* type and that the relative proportion of Mg : Ti on the *T* sites increases very little over the solid-solution range. Constrained Rietveld refinement of the present data, in which the overall Mg : Ti ratio was fixed and the relative proportion of Mg : Ti on each site was allowed to vary, did not provide any conclusive evidence of preferential occupancy. Although the Bragg *R* factor of the neutron data is sensitive to changes in the overall Mg : Ti ratio, it is somewhat insensitive to the relative proportions on each site given a fixed overall ratio. This was also found to be the case in monoclinic $Ba_{1\cdot27}(Fe_{2\cdot54}Ti_{5\cdot46})O_{16}$ (Cheary, 1986).

Support for preferential occupancy at $x = 1{\cdot}33$ is given by other changes in the structural parameters. In particular, the cation–cation separation ($B1_1$–$B1_2$) within the wall of *S* octahedra increases from 2·973 (8) Å at $x = 1{\cdot}14$ to 3·008 (8) Å at $x = 1{\cdot}33$, reflecting an increased proportion of larger octahedral cations within the wall. The corresponding separation in the *T* wall ($B2_1$–$B2_2$) undergoes very little change [*i.e.* from 2·978 (8) to 2·973 (8) Å]. In addition, the distance between the tunnel axis and the Ol_4 (or Ol_3) oxygens in the centre of an *S* wall decreases by 0·02 to 2·548 Å at $x = 1{\cdot}33$ whilst the decrease in separation between the $O4_3$ or $O4_4$ oxygens in a *T* wall and the tunnel axis is only 0·002 Å. The relevance of these dimensions in the present context follows from the fact than an increased proportion of Mg^{2+} ions in an *S* wall will make the repulsive component of the electrostatic force between the octahedral cations and the bariums in the tunnel smaller than the corresponding repulsion with the *T* wall. The overall attraction between an *S* wall and the Ba ions, which is dominated by the Ba–O attraction, will therefore be enhanced by a higher proportion of Mg^{2+} ions in the *S* walls.

An estimate of the Mg/Ti ratio on the *S* and *T* sites can be made if it is assumed that the difference in the observed Mg/Ti–O bond lengths arises solely from preferential occupancy. The overall average bond length $\langle D \rangle$ represents a weighted average of the Mg–O (D_{Mg}) and the Ti–O (D_{Ti}) bond lengths. For xBa per unit cell this is given by

$$\langle D \rangle = (x/8)D_{Mg} + [1-(x/8)]D_{Ti}. \quad (1)$$

When the overall bond lengths $\langle D \rangle$ at $x = 1{\cdot}14$ and 1·33 in Table 2 are substituted into (1), this gives $D_{Mg} = 2{\cdot}1089$ Å and $D_{Ti} = 1{\cdot}9535$ Å. These values can then be used to evaluate the relative proportions of Mg and Ti on the *S* and *T* sites of the $x = 1{\cdot}33$ hollandite using a modified form of equation (1), namely,

$$\langle D \rangle = \beta D_{Mg} + (1-\beta)D_{Ti} \quad (2)$$

where $\langle D \rangle$ is now the average on a particular site (*S* or *T*) and β is the fraction of these sites filled with Mg ions. This analysis indicates that the Mg : Ti ratio in the 1·33 hollandite is 1 : 4·6 on the *S* sites and 1 : 5·5 on the *T* sites. Random occupancy corresponds to a ratio of 1 : 5.

The octahedral cations also appear to play a role in the ordering of the tunnel ions. In many hollandites long-range, one-dimensional ordering occurs along the tunnels. In most barium hollandites $Ba_x(M_yTi_{8-y})O_{16}$ there is correlation between tunnels and the ordering is three dimensional. The lateral extent of the correlation between adjacent tunnels varies with the choice of *M* ion. For $M = Mg^{2+}$ or Ti^{3+} well-resolved superlattice lines are observed (Bursill & Grzinic, 1980; Kesson & White, 1986*b*), but with $M = Al^{3+}$ the superlattice lines are broadened and remain so even after extensive annealing (Cheary, Hunt & Calaizis, 1981). Kesson & White (1986*b*) have suggested that three-dimensional ordering is controlled by the degree of electrostatic shielding presented by the tunnel walls. In their model the electronic polarizability of the octahedral cations is the source of the shielding. It is proposed here that the polarization arises not from electronic polarization, but from permanent dipole moments set up by the off-centring of the octahedral cations in the oxygen octahedra. This off-centring arises from the electrostatic repulsion between the adjacent columns of cations within each wall. In each unit cell eight dipoles are formed, but the overall dipole moment per unit cell is zero. With this arrangement an attractive force is set up between the dipoles in each wall and the columns of Ba ions on each side of the wall (see Fig. 4), and an electrostatic shield is created which partially cancels the repulsive Ba–Ba interaction between neighbouring tunnels. When the Ba–Ba interaction is weakened by off-centring, three-dimensional ordering will tend to be

short range. In $Ba_{1\cdot14}(Al_{2\cdot28}Ti_{5\cdot72})O_{16}$ the average off-centre shift of the Al/Ti ions is 0·13 Å (Cheary, 1986, 1987) and the coherence distance T of the ordering, calculated from the instrumentally corrected full-width-at-half-maximum intensity (*i.e.* FWHM = $\lambda/T\cos\theta$) of the strongest superlattice line, is approximately 40 Å. In the corresponding Ba(MgTi) hollandite, the average off-centre shift is 0·08 Å and the coherence length is 270 Å. The extent of the three-dimensional ordering in these compounds appears to have some form of inverse relation with the off-centre shift. Examination of the breadths of superlattice lines from a range of Ba hollandites with various 2+ and 3+ octahedral cations replacing Mg indicates a strong correlation between three-dimensional ordering and the ionic radius of the ion included with Ti on the B sites. Further studies of this aspect of ordering are in progress.

In Ba_x(Mg/Ti) hollandites, commensurate superstructures have been identified at $x = 1\cdot2$ and 1·333 (Bursill & Grzinic, 1980). At all other compositions the ordering is incommensurate. Ordering in the present hollandites has been examined by monitoring the 2θ position of the second strongest superlattice line in the X-ray powder pattern as this is the only one visible at all x. The line used actually consists of two closely spaced lines which can be indexed on a monoclinic hollandite unit cell as the $0k1$ and $1k0$ lines. In this representation the values of k at the commensurate superstructure compositions $x = 1\cdot2$ and 1·33 are 0·6 and 0·6667, respectively. This k index is related to the multiplicity m normally used to describe superlattices in hollandites by the relation $m = 2/(1-k)$. Fig. 5 shows the effect of the Ba concentration on the 2θ position of the superlattice line. Over the solid-solution range the actual movement of the superlattice line is almost linear and a sensitive indicator of the Ba concentration. The theoretical line shown in Fig. 5 is based on the change in 2θ being linear over the solid-solution range and is simply the line drawn between the mean 2θ calculated for the $0k1/1k0$ pair at $x = 1\cdot2$ and 1·333 using the appropriate lattice parameters and assuming the normal superstructures associated with these compositions (*i.e.* Ba–Ba–Vacancy–Ba–Vacancy for $x = 1\cdot2$ and, Ba–Ba–Vacancy for $x = 1\cdot33$). At $x = 1\cdot2$ the calculated 2θ position agrees well with experiment, but either side of this value theory and experiment follow distinctly different trends. At $x = 1\cdot33$ the observed multiplicity m is $5\cdot85 \pm 0\cdot05$ rather than the expected value of 6. This discrepancy is significant and has been observed previously by Bursill & Grzinic (1980) who reproducibly obtained multiplicities from electron diffraction patterns between 5·80 and 5·90 in both $Ba_{1\cdot33}(Mg_{1\cdot33}Ti_{6\cdot67})$ and $Ba_{1\cdot33}(Ga_{2\cdot66}Ti_{5\cdot34})$ hollandites. The observed multiplicity of $4\cdot73 \pm 0\cdot05$ at the $x = 1\cdot14$ end in the present data is also different from the calculated value, but is similar to the electron diffraction value, $m = 4\cdot70$.

Despite the large discrepancy at $x = 1\cdot33$, high-resolution microscopy indicates that Ba–Ba–Vacancy ordering does occur, but only over local regions or domains 60–90 Å across. Within each region or domain the structure is the same and at the boundary a phase shift occurs in the supercell origin (*e.g.* the superstructure changes from Ba–Ba–Vacancy to Ba–Vacancy–Ba). It would appear therefore that the deviation from $m = 6$ condition is related to the formation of these domains and the effect a high proportion of boundaries has on the superstructure periodicity. This is probably true also of the 1·14 end, as domains have also been observed near this composition (Fanchon *et al.*, 1987). The diffraction theory for determining the effect of domain boundaries on the 2θ positions of the superlattice lines is being investigated,

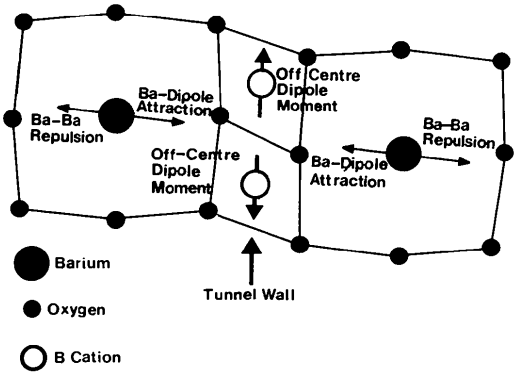

Fig. 4. Model of screening between tunnels arising from the off-centring of B ions in the tunnel walls. Screening is more effective when the off-centre dipole moment is large.

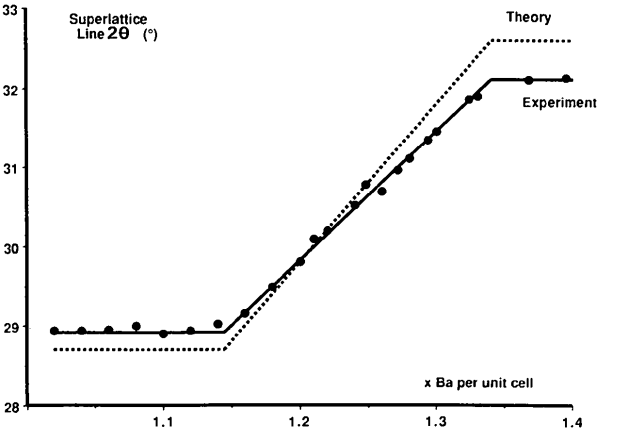

Fig. 5. Comparison of the observed and theoretical 2θ positions of the $0k1/1k0$ superlattice line using Cr $K\alpha$ radiation. The theoretical plot was formed by drawing a line through the 2θ positions corresponding to the commensurate superstructures at $x = 1\cdot2$ and 1·33 and extending this between the limiting composition $x = 1\cdot14$ and 1·33.

with the possible boundary types being determined by the constraint that vacancies never exist as nearest neighbours along the tunnels (Mijlhoff *et al.*, 1985; Kesson & White, 1986*a*). Further experiments are being carried out to investigate the effect of annealing on the growth of these domains.

We wish to acknowledge the support given to this work by the Australian Nuclear Science and Technology Organization (Research Contract No. 82/X/1) and the Australian Institute of Nuclear Science and Engineering.

References

BURSILL, L. A. & GRZINIC, G. (1980). *Acta Cryst.* B**36**, 2902–2913.
BYSTRÖM, A. & BYSTRÖM, A. M. (1950). *Acta Cryst.* **3**, 146–154.
CADEE, M. C. & VERSCHOOR, G. C. (1978). *Acta Cryst.* B**34**, 3554–3558.
CHEARY, R. W. (1986). *Acta Cryst.* B**42**, 229–236.
CHEARY, R. W. (1987). *Acta Cryst.* B**43**, 28–34.
CHEARY, R. W., HUNT, J. V. & CALAIZIS, P. (1981). *J. Aust. Ceram. Soc.* **17**, 11–12.
DRYDEN, J. C. & WADSLEY, A. D. (1958). *Trans. Faraday Soc.* **54**, 1574–1580.
FANCHON, E., VICAT, J., HODEAU, J. L., WOLFERS, P., TRAN QUI, D. & STROBEL, P. (1987). *Acta Cryst.* B**43**, 440–448.
HOWARD, C. J. (1982). *J. Appl. Cryst.* **15**, 615–620.
HOWARD, C. J., BALL, C. J., DAVIS, L. D. & ELCOMBE, M. M. (1983). *Aust. J. Phys.* **35**, 507–518.
HOWARD, C. J. & HILL, R. J. (1986). Australian Atomic Energy Commission Report, Lucas Height Research Laboratories. AAEC/M112.
KESSON, S. E. (1983). *Radioact. Waste Manage.* **4**, 53–72.
KESSON, S. E. & WHITE, T. J. (1986*a*). *Proc. R. Soc. London Ser. A*, **405**, 73–101.
KESSON, S. E. & WHITE, T. J. (1986*b*). *Proc. R. Soc. London Ser. A*, **408**, 295–319.
MIJLHOFF, F. C., IJDO, D. J. W. & ZANDERBERGEN, H. W. (1985). *Acta Cryst.* B**41**, 98–101.
POST, J. E., VON DREELE, R. B. & BUSECK, P. R. (1982). *Acta Cryst.* B**38**, 1056–1065.
ROTH, R. (1981). Annual Report, National Measurements Laboratory, Office of Nuclear Technology. NBSIR 81-2241.
WEBER, H. P. & SCHULTZ, H. (1986). *J. Chem. Phys.* **85**, 475–484.
WILES, D. B. & YOUNG, R. A. (1981). *J. Appl. Cryst.* **14**, 149–150.

Acta Cryst. (1989). B**45**, 212–218

Structure of ND_4F-II

BY A. C. LAWSON AND R. B. ROOF

Los Alamos National Laboratory, Los Alamos, New Mexico 87545, *USA*

J. D. JORGENSEN

Argonne National Laboratory, Argonne, Illinois 60439, *USA*

AND B. MOROSIN AND J. E. SCHIRBER

Sandia National Laboratories, Albuquerque, New Mexico 87185, *USA*

(*Received* 21 *July* 1988; *accepted* 3 *January* 1989)

Abstract

The crystal structure of ND_4F-II has been determined at 4·69 kbar ($4{\cdot}69 \times 10^5$ kPa) at room temperature [$a_{II} = 8{\cdot}508(1)$, $c_{II} = 16{\cdot}337(2)$ Å, $V = 1024{\cdot}1(2)$ Å^3, $R_{wp} = 2{\cdot}91\%$ for 250 reflections]. The structure is rhombohedral, space group $R3c$, with 24 molecules per hexagonal unit cell. Like its parent phase, ND_4F-I with the hexagonal wurtzite structure, it consists of corner-sharing tetrahedral units. However, it has a structure that is topologically distinct from that of the ND_4F-I phase and that accounts for the 28% volume collapse observed at the I–II transition. The transition is accomplished by filling the empty space in the parent structure, with reductions in the volumes of the tetrahedral units of only 2·4–5·2%. The ND_4F-II phase was found to be stable down to at least 50 K, and its thermal expansion was determined. The anisotropic compressibility of the ND_4F-I phase at room temperature is also reported.

Introduction

Under ordinary conditions of temperature and pressure NH_4F has the wurtzite structure (Zachariasen, 1927). It is useful to visualize this structure in terms of hexagonally close-packed layers of F atoms that give rise to a network of corner-sharing tetrahedra. The NH_4^+ ions fit nicely into alternate tetrahedra, and a nearly perfect tetrahedral arrangement of N–H–F hydrogen bonds is achieved (Adrian & Feil, 1969; Morosin, 1970). The resulting structure does not fill space very efficiently, as the fraction of space filled by

0108-7681/89/030212-07$03.00